JOURNAL OF MATERIALS SCIENCE 20 (1985) 2913–2922

Mechanical properties and deformation behaviour of some zirconium–nickel amorphous alloys

G. K. DEY, S. BANERJEE
Physical Metallurgy Division, Bhabha Atomic Research Centre, Bombay 400 085, India

A series of zirconium–nickel alloys have been melt-spun under identical conditions to produce partly crystalline and fully amorphous ribbons. The mechanical properties: hardness and fracture strength of these ribbons have been determined. The deformation and fracture behaviour in bending and tension have been studied and the effect of the crystalline particles on the deformation and fracture processes has been examined. The structure of the deformation defects has also been investigated.

1. Introduction

In recent times, metallic glasses have emerged as a new class of material. Because of their ultra-high strength, isotropic elastic properties and unique deformation behaviour, all significantly different from those of crystalline metallic materials, studies on the mechanical properties of metallic glasses have attracted wide attention in recent years.

Extensive research has been done to study flow and fracture in metal–metalloid glasses. Investigations on the deformation behaviour of metal–metal glasses, however, have not been so extensive. The hardness of some of the titanium-based and zirconium-based metal–metal glasses has been determined by some investigators [1, 2]. This paper reports some mechanical property data for zirconium–nickel partly crystalline and fully amorphous glasses and some features of their deformation behaviour.

Some investigators have reported higher strength and ductility in melt-spun ribbons containing a certain optimum volume fraction of crystalline particles formed either during rapid solidification by melt-spinning or by crystallization subsequent to melt-spinning [3–6]. A comparison of mechanical properties and processes of deformation and fracture under tension of partly crystalline and fully amorphous ribbons containing different amounts of nickel has been made in the present work in order to evaluate the effects of the crystalline particles and of solute content on the deformation and fracture behaviour or Zr–Ni glasses.

In spite of the homogeneous structure of metallic glasses, the deformation process in these has been found to have a component that is non-homogeneous on a scale as coarse as several hundred times the interatomic spacing. The major part of the plastic deformation in a metallic glass is localized within the shear bands [7, 8]. Several investigations have been directed towards resolving the "structure" within the shear bands, but an unequivocal description of such a structure has not been arrived at so far. There have also been some attempts to investigate whether shear bands provide preferential sites for crystallization in samples undergoing crystallization subsequent to deformation. Donovan *et al.* [9] have observed that in Ni–P glass, crystallization proceeded at the same rate at shear bands as at regions free from bands. The possibility of the bands acting as preferred sites for the nucleation of crystals during crystallization in deformed specimens has been examined in this paper.

0022–2461/85 $03.00 + .12

2. Experimental details

Crystal bar zirconium and high-purity nickel were melted in an arc furnace under an argon atmosphere to produce alloy buttons of the following compositions: Zr–24 at % Ni, Zr–33 at % Ni, Zr–35 at % Ni and Zr–39 at % Ni.

The buttons were remelted several times for homogenization. Pieces of the alloy buttons were melt-spun in a melt-spinning device. The speed of revolution of the wheel and other parameters like ejection pressure, wheel–nozzle distance and nozzle shape were identical for all compositions. The ribbons produced were about 2 mm wide and 30 μm thick. X-ray diffraction on the ribbons was carried out on the wheel side (surface in contact with the wheel during melt-spinning) as well as on the air side (surface away from the wheel side).

Thin foils for electron microscopy were prepared by using an electrolyte comprising 300 ml of methanol, 165 ml of n-butanol and 35 ml of perchloric acid. The temperature of the electrolyte was kept below 220 K by using a bath containing dry ice and methanol.

Tensile testing was carried out in a universal testing machine at a strain rate of $1 \times 10^{-3}\,\mathrm{min}^{-1}$. Microhardness was measured using a 100 g load. Scanning and transmission electron microscopy (SEM and TEM) were used to study the morphology of the fracture surface and the deformation band structure.

3. Results and discussion

3.1. Melt quenched structure

X-ray diffraction carried out on the air side surface of the tapes revealed that the Zr–24 at % Ni composition was partly crystalline. The other compositions were found to be fully amorphous. X-ray diffraction on the wheel side surface showed identical results.

The wheel side surfaces of the ribbons were examined by SEM. The surfaces were found to have air pockets (Fig. 1). These are depressions which form due to entrapment of air in the puddle formed on the wheel during melt-spinning. A detailed mechanism of formation of these defects has been discussed elsewhere [10].

Thin foils of a ribbon of Zr–24 at % Ni alloy showed crystals distributed in an amorphous matrix. The volume fraction of the crystalline phase was found to be around 40%. A thinner tape (20 μm thick) of the same composition was found to be fully amorphous. No crystalline particles, however, could be seen in thin foils of ribbons of other compositions. An electron diffraction pattern and a micrograph of Zr–35 at % Ni ribbon representing the typical amorphous structure are shown in Figs. 2a and b.

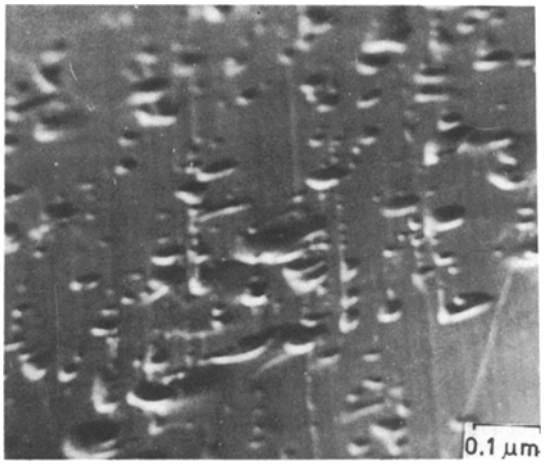

Figure 1 Air pockets on the wheel side surface in a Zr–33 at % Ni ribbon.

3.2. Mechanical properties

The hardness, fracture strength and ratio of these two quantities for ribbons of different compositions are shown in Table I. Indentations for hardness measurement were made on the wheel side surface of electro-polished ribbons. In the partly crystalline specimens, the indentations were made on regions free from crystals. The hardness values thus correspond to those of the amorphous phases in all compositions.

Specimens for tensile testing had a 5 mm gauge length. The gauge length was polished to give it a reduced cross-section. This procedure ensured failure in the gauge length and prevented premature failure at the grips. Polishing the gauge length also removed air pockets. The presence of these defects is likely to result in stress concentration and failure at such defects, yielding an incorrect value for the strength.

Sargent [11] and others [12, 13] have proposed empirical relationships between hardness and fracture stress or yield stress which hold for nearly all metallic glasses. The ratio of hardness to fracture strength of 3.6 observed in Zr–Ni glasses has been found to be very close to that observed in other metallic glasses and considerably different from that observed in silicate glass [13].

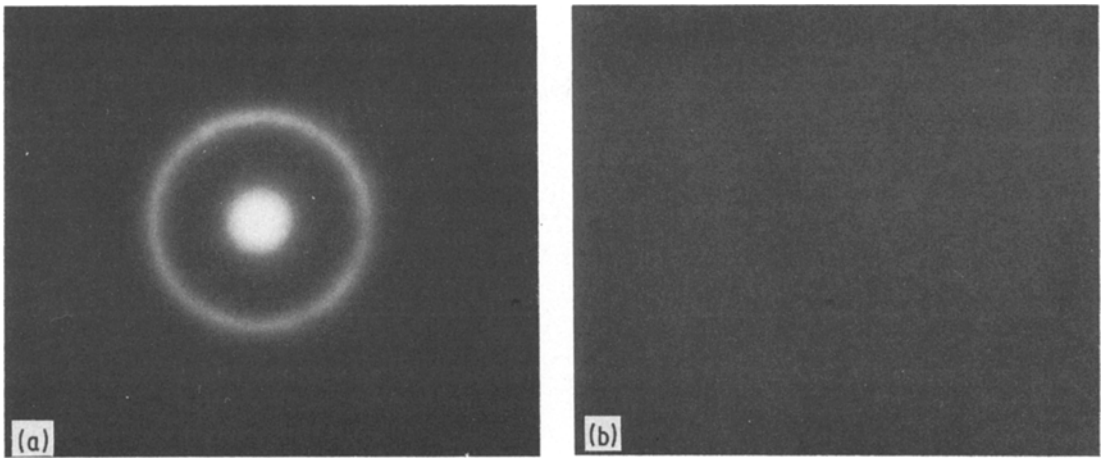

Figure 2 (a) Electron diffraction pattern and (b) bright-field electron micrograph from the amorphous structure in a Zr–35 at % Ni ribbon.

The hardness as well as the fracture strength were found to increase with nickel content. An increase in hardness with nickel content has also been observed by Zielinski *et al.* [1]. The hardness values compared favourably with those reported there [1]. A comparison of the strength and hardness of these glasses with those of commercial crystalline alloys of zirconium, Zircaloy-2 and Zr–2.5Nb [14, 15], used as structural materials in nuclear reactors, shows that the former are stronger and harder but are less ductile in tensile loading.

3.3. Deformation behaviour

3.3.1. Tensile deformation

Typical engineering stress–elongation curves for ribbons of different compositions are shown in Fig. 3. The fully amorphous compositions showed small amounts of plastic deformation before fracture. The partly crystalline compositions, however, showed no plastic deformation prior to fracture. The tensile strength was also found to be lower compared to that of fully amorphous compositions. An increase in strength due to the presence of crystalline particles in an amorphous matrix (compared to a fully amorphous specimen) has been indicated in some studies [3–6]. However, the presence of only the optimum quantity of crystalline particles results in increased strength. The increase in strength due to the presence of a dispersed crystalline phase in an amorphous matrix was also found to be associated with enhanced ductility. The optimum volume fraction of crystalline phase required to give enhanced strength and ductility has been found to be 0.31 in $Fe_{70}Ni_{20}Zr_9Nb_1$ alloy [3]. A volume fraction higher than the optimum value leads not only to loss of ductility but also to loss of strength [3]. The volume fraction of crystalline particles in the partly crystalline ribbon of Zr–24 at % Ni was found to be around 40%. The lack of ductility in this partly crystalline ribbon appears to be due to the fact that the volume fraction of crystalline phase exceeded the optimum value. The lower strength could be due to a non-optimum crystalline particle content as well as to lower nickel content of this composition. Fully amorphous ribbons of this composition obtained by melt-spinning under a different set of melt-spinning conditions showed higher strength and ductility (see Table I and Fig. 3). It can thus be inferred that the low strength of the partly crystalline ribbons was primarily due to the presence of a non-optimum volume fraction of crystalline phase.

TABLE I Mechanical properties of amorphous Zr–Ni alloys

Alloy composition	Hardness, H ($kg\,mm^{-2}$)	Fracture stress, σ_f (MPa)	H/σ_f
Zr–24 at % Ni*	522	1324	3.86
Zr–24 at % Ni	522	1373	3.72
Zr–33 at % Ni	537	1432	3.67
Zr–35 at % Ni	552	1491	3.63
Zr–39 at % Ni	568	1569	3.55

*Partly crystalline

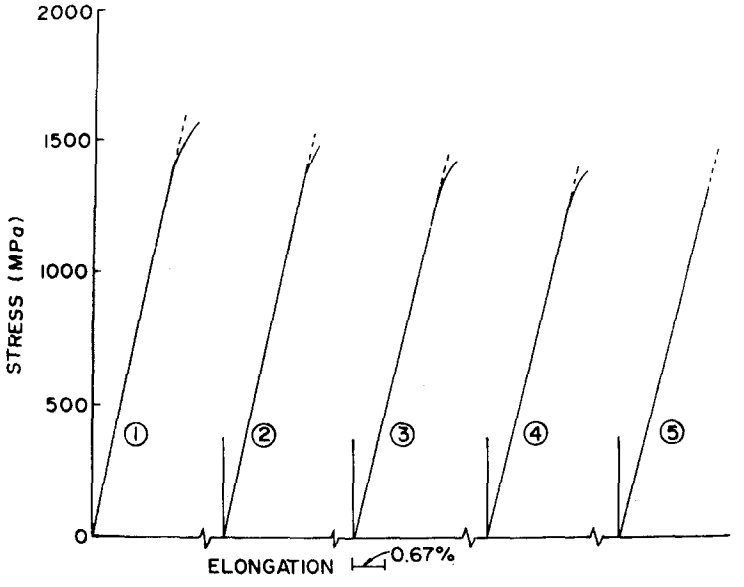

Figure 3 Nominal stress–elongation curves for ribbons of different compositions: (1) Zr–39 at % Ni; (2) Zr–35 at % Ni; (3) Zr–33 at % Ni; (4) Zr–24 at % Ni; (5) Zr–24 at % Ni, partly crystalline.

The surfaces of tensile specimens were observed after giving them different amounts of deformation. Shear bands were found to develop on the surface (Fig. 4). The density of the bands seemed to increase with increased deformation.

3.3.2. Deformation under bending

The ribbons were deformed by bending them over the edge of a razor blade. The ribbons could be bent through 180° without any sign of brittleness. Fig. 5 shows large-scale shear band formation on the outer side (the side experiencing tensile deformation) of the bent specimen. The shear bands can be seen to go deep into the specimen. The distance between the bands was found to increase away from the bend.

The appearance and density of the shear bands were not influenced by the nature of the surface (i.e. wheel or air side) or by the presence of crystalline particles in the specimens. The right type of distribution of crystalline particles in metallic glasses like $Fe_{84}B_{16}$ has been found to reduce the average spacing between adjacent shear bands and as a result there is an improvement in ductility [6]. The observation that the shear bands are not more closely spaced in partly crystalline Zr–24 at % Ni alloy is consistent with the fact that this alloy did not exhibit

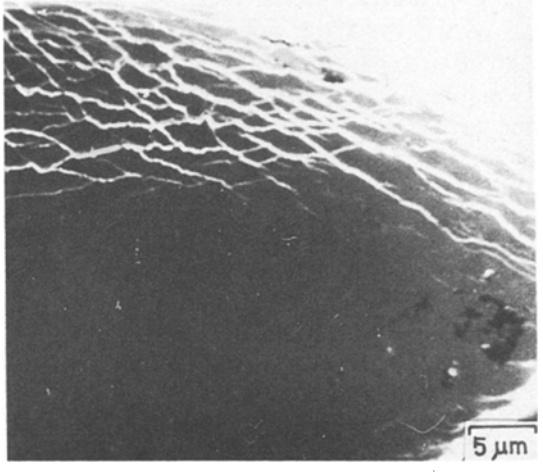

Figure 4 Shear bands on the surface of a Zr–35 at % Ni ribbon after tensile deformation.

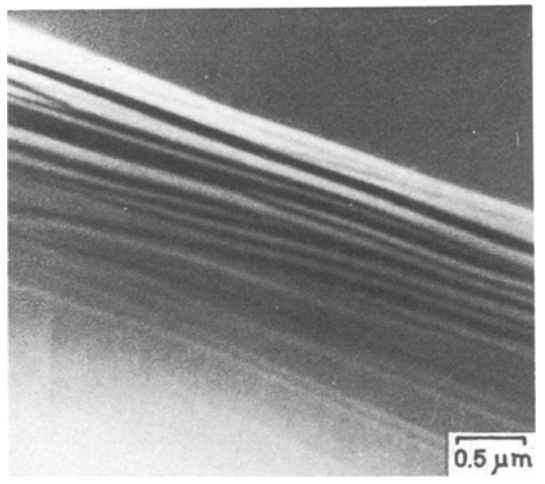

Figure 5 Shear bands on the outer side of the bent specimen. The distance between the bands is increasing away from the bend. Specimen from a Zr–35 at % Ni ribbon.

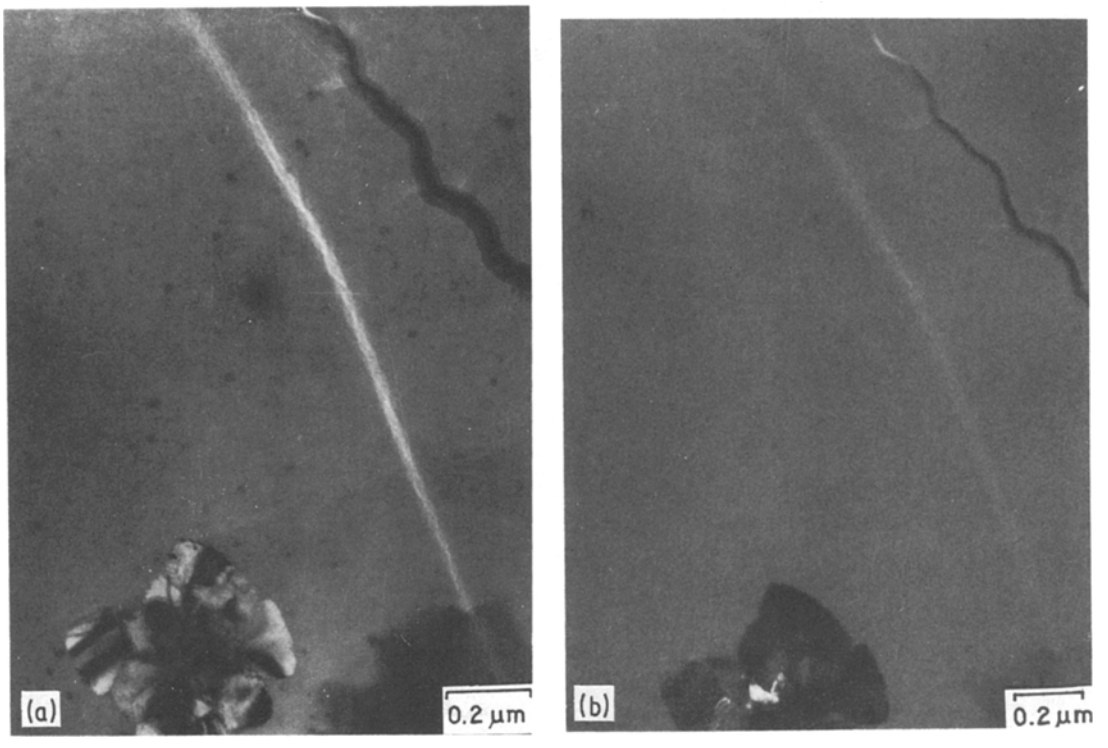

Figure 6 (a) Bright-field and (b) dark-field electron micrographs showing a band in a deformed Zr–24 at % Ni alloy. The feature in the top right-hand corner is a crack. The crack tip also has a band-like contrast. An aggregate of crystals can be seen at the bottom.

any improved ductility in comparison with those of fully amorphous alloys richer in nickel.

3.4. Structure of deformation defects

Several investigations have been carried out to understand the structure of shear bands [9, 16–18]. The general conclusion arrived at has been that, in thin foils prepared for TEM, these are regions of reduced thickness. It has also been proposed that these regions diffract in a manner different from amorphous regions free from such defects [9].

Fig. 6a shows a TEM bright-field image of shear bands formed in a sample subjected to tensile deformation. It can be seen that the defect shows up as a bright line against the background. The length of the lines did not exceed a few micrometres and the lines were typically about 25 to 30 nm wide. A through focal series observation showed that, although the coarseness of the granularity changed, there was no change in width of the defects. A through focus observation was essential because the defects are observed only as a change in contrast of the granularity, and granularity is a phase effect [16]. Dark-field micrographs taken with the aperture centred on the first diffraction halo (Fig. 6b) showed the band to be of higher intensity. The contrast was identical to that observed in bright-field. This evidence suggested that the bands were regions of reduced thickness.

A junction of shear bands is shown in Fig. 7a. Careful observation of the extended parts of the junction revealed that the main band had branches emanating from it. This indicated the possible presence of stress concentration close to the band. Some regions of the band were found to be darker than the rest. No reversal of contrast was observed in dark-field micrographs obtained by placing an aperture on the first diffraction halo (Fig. 7b). The bright-field and dark-field observations of the junction of shear bands also indicated that these are regions of reduced thickness. Figs. 7a and b also show small crystals that formed by crystallization due to prolonged heating by the electron beam in the electron microscope. The nucleation of crystals was found to be homogeneous and the shear bands did not act as preferential sites for

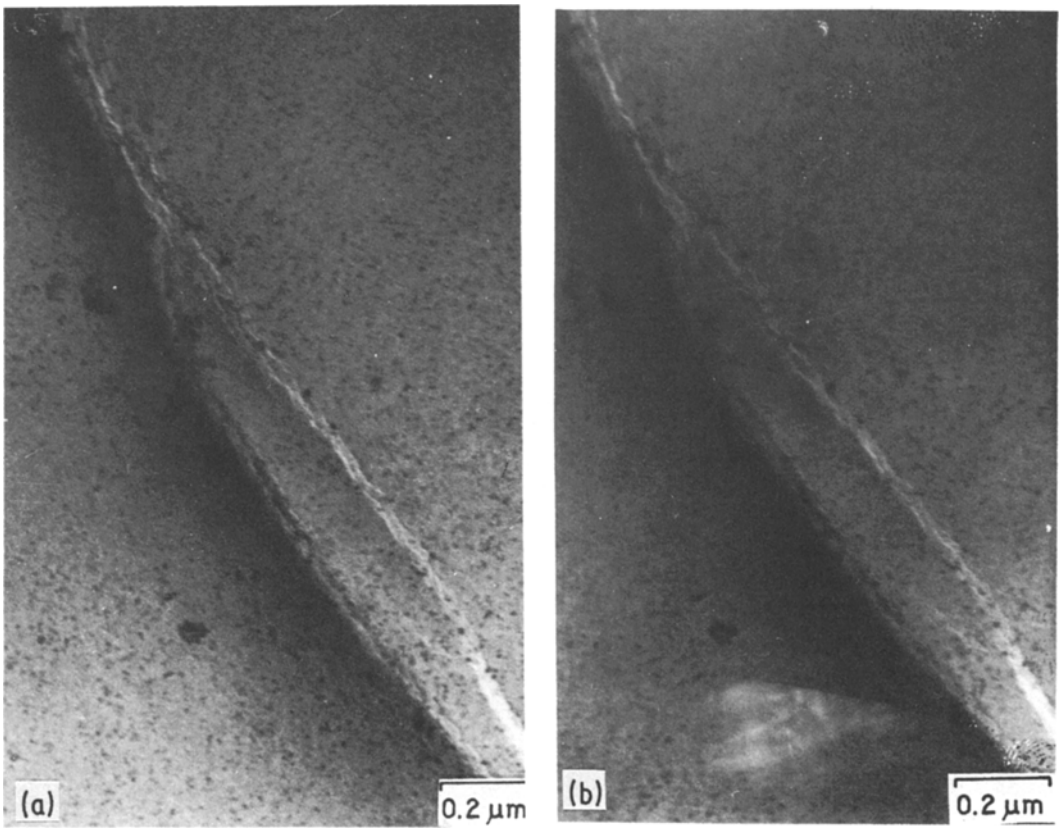

Figure 7 (a) Bright-field and (b) dark-field electron micrographs showing a junction of bands. A few large crystals and a high density of small crystals can also be seen. Specimen from a Zr–39 at % Ni ribbon.

nucleation. In this regard, the observations were similar to those of Donovan *et al.* [9]. Donovan *et al.* [9] have also observed that, in dark-field electron micrographs formed by electrons scattered within the first diffraction halo, shear bands sometimes show more intense specks than does the rest of the region, suggesting that the bands not only are regions of reduced thickness but also possess a different scattering behaviour. In the present study, however, no such effect was observed.

Thin foils prepared from the bent regions showed deformation bands identical to those observed in specimens subjected to tensile deformation.

The appearance of the bands as regions of reduced thickness in tensile as well as bent specimens examined in TEM was indicative of preferential attack of the electro-polishing solution used for thin foil preparation. Consideration has been given to the factors contributing to such a preferential attack at the bands [17, 18]. It is believed that, since chemical and topological order of atomic arrangements are different at shear bands, these show a different response to the electro-polishing solution. However, the exact nature of the difference in chemical and topological order between the bands and amorphous regions free from such bands has not yet been defined.

In view of such differences in the state of order between the shear bands and the amorphous matrix, it was expected that the former would act as preferential nucleation sites for crystallization in a manner similar to heterogeneous nucleation of precipitates on dislocations. The present observations, however, have revealed that no such preferential nucleation of precipitates occurs on shear bands. A satisfactory explanation of this observation cannot be given at this stage.

It is interesting to note that the number density of shear bands produced in Zr–Ni glass samples after the small macroscopic deformation that these samples can take before fracture has been found to be orders of magnitude

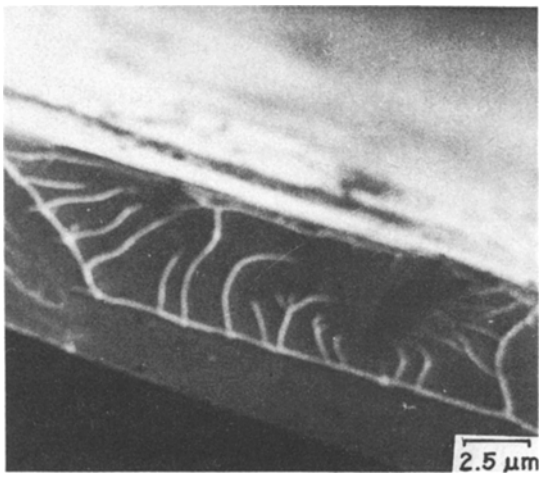

Figure 8 Fracture surface for a fully amorphous ribbon (Zr–35 at % Ni). The flat region at the bottom is the region of shear. The region at the top shows an extensive vein pattern.

lower than that of dislocations (10^7 to $10^8\,cm^{-2}$) even in annealed crystalline alloys. This suggests a much larger displacement field associated with the shear bands than that for individual dislocations.

3.5. Fracture morphology

3.5.1. Fracture under tension

Tensile deformation was found to result in fracture of the specimen with or without very small overall plastic deformation. The fracture surface was found to be inclined to the tensile axis at an angle of approximately 45° in partly crystalline as well as fully amorphous specimens. The shear stress is expected to be a maximum on planes with such an inclination. Fig. 8 shows the fracture surface of a fully amorphous specimen. The fracture surface consists of two distinct regions: a flat featureless region close to one surface of the ribbon and the other region showing extensive vein structure. The region with the vein structure extended up to the other surface of the ribbon. The occurrence of fracture is represented schematically in Fig. 9. It can be observed that the flat featureless region originates due to shear whereas the vein pattern is a result of necking taking place after shear. Because of the sequential nature of the two processes, the two fracture surfaces are not mirror images of each other. The appearance of the fracture surface was found to be typical of any amorphous alloy. Though the specimens did not show any appreciable amount of macroscopic ductility, the fracture surface did not bear any resemblance to the fracture surfaces of brittle materials. The vein patterns showing extensive necking were a manifestation of enormous plastic deformation on a microscopic scale. The orientation of the fracture surface and the fact that the two complementary surfaces were not mirror images on a microscopic scale also supported the non-brittle nature of the fracture [19]. There was evidence of large-scale necking on the fracture surface. A careful examination (Fig. 10) showed ridges created by necking. The triple-point junction of the ridges, in many cases, was found to be the origin of long tapering filaments (Fig. 11). These filaments had tapered due to extensive plastic deformation followed by rupture.

In the partly crystalline specimens, the crystalline particles did not lower the ductility at the fracture surface. The fracture surface resembled that obtained in fully amorphous ribbons,

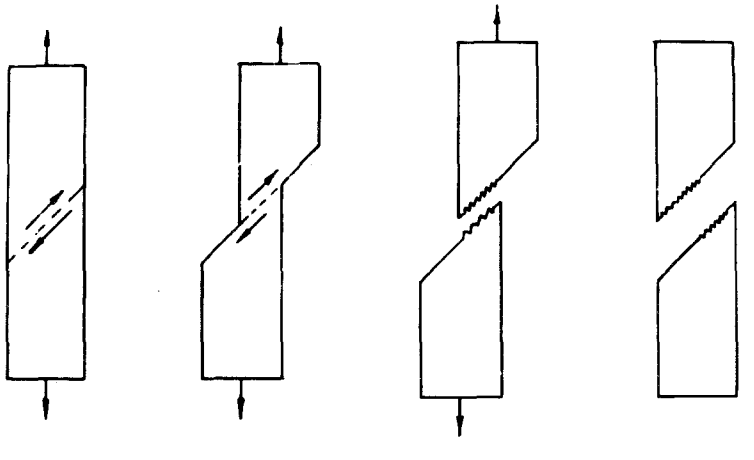

Figure 9 Schematic representation of the process of fracture by shear followed by necking.

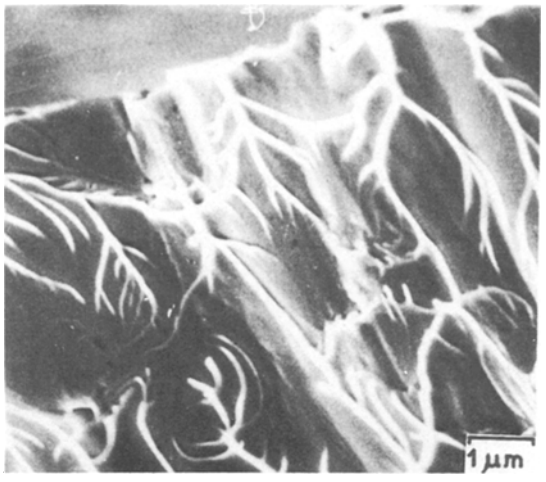

Figure 10 Ridges created by necking on the fracture surface in a Zr–33 at % Ni ribbon.

except for the presence of some voids and cavities. It was found that the deformation leads to crack or void formation at the crystal/amorphous matrix interface. Fig. 12 shows a TEM micrograph of the partly crystalline ribbon before deformation, illustrating a crystal in the amorphous matrix. It can be seen that the crystal/amorphous matrix interface does not show any crack or discontinuity. The structure obtained after deformation can be seen in Fig. 13. This micrograph shows large cracks at the crystal/amorphous matrix interface. The crystalline particles did not show any dislocation structure, indicating that these particles did not undergo plastic deformation to any significant extent. This observation is in keeping with the fact that the crystals are of intermetallic compounds, which are generally very difficult to

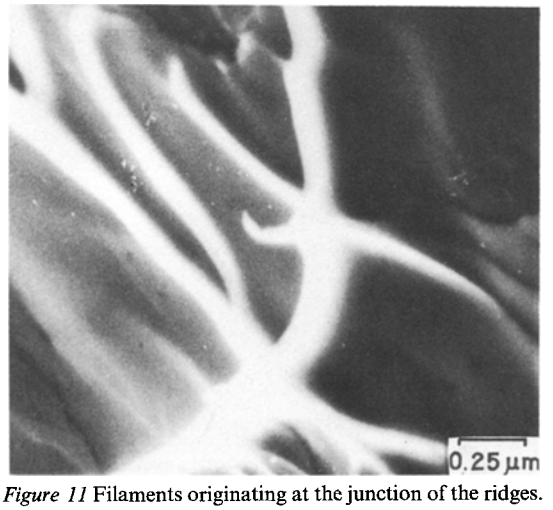

Figure 11 Filaments originating at the junction of the ridges.

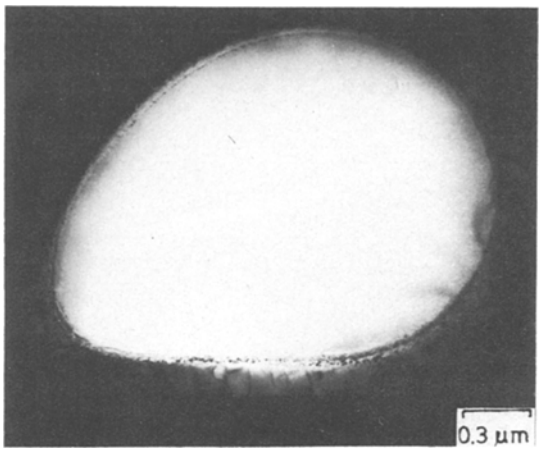

Figure 12 Bright-field electron micrograph of partly crystalline Zr–24 at % Ni ribbon before deformation, showing a crystal in the amorphous matrix. No cracks can be seen at the crystal/amorphous matrix interface.

deform. It should be mentioned here that, of the very large number of crystal/amorphous matrix interfaces examined, not all showed cracks (e.g. the crystal/amorphous matrix interface in Figs. 6a and b). No apparent interaction between the shear bands and the crystalline particles could be observed.

3.5.2. Fracture by bending

Fracture by bend deformation was brought about by repeatedly bending and unbending the ribbons. It was possible to give four to five such cycles of deformation to the fully amorphous ribbons before fracture occurred. However, the partly crystalline ribbons could withstand only one or two such cycles.

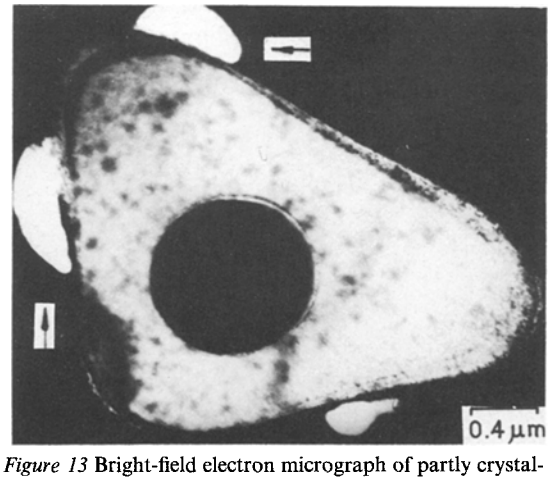

Figure 13 Bright-field electron micrograph of partly crystalline Zr–24 at % Ni ribbon after deformation. Arrows indicate cracks at the crystal/amorphous matrix interface.

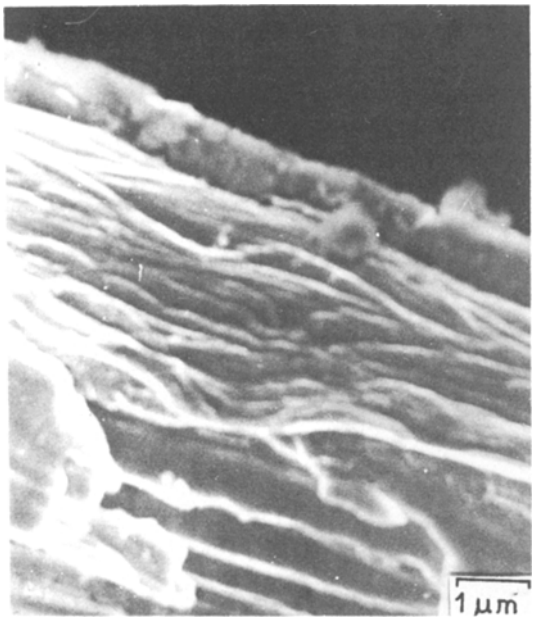

Figure 14 Fracture surface obtained by repeated bending of a Zr–33 at % Ni ribbon. Long ridges running across the width of the specimen can be seen.

The fracture surfaces obtained were completely different from those obtained under tension (Fig. 14). No vein patterns could be seen; instead, long ridges running across the width of the specimen were observed. Alternate tensile and compressive deformation appears to have generated persistent deformation bands along the axis of bending and the deformation remains essentially localized within these deformation bands. As a consequence, ridges, which are the last regions to be detached, appear on the fracture surface along the bending axis. The fracture surfaces in partly crystalline ribbons were found to be identical to those of fully amorphous ribbons, suggesting that the directionality introduced by this cyclic bending process is so strong that the distribution of hard second-phase particles has practically no influence on the mode of deformation and fracture.

4. Conclusions

Based on the different aspects of this study the following conclusions can be arrived at:

(a) The hardness and strength of the amorphous ribbons were found to increase with nickel content in the composition range studied.

(b) The presence of about 40% of crystalline particles reduced the strength and ductility of Zr–24 at % Ni ribbons as compared to fully amorphous ribbons of the same composition.

(c) In ribbons of all compositions, fracture in tension was found to occur by local plastic deformation, followed by necking and rupture.

(d) Fracture in bending was by formation of deformation bands along the bending axis.

(e) The shear band contrast observed in TEM is due to the reduced thickness of shear band regions in thin-foil specimens.

Acknowledgements

The authors are grateful to Dr M. K. Asundi for his keen interest in the work. Assistance in experimentation by Mr. S. L. Wadekar and R. T. Savalia is gratefully acknowledged. The authors are also indebted to Mr E. G. Baburaj for his help in preparation of the metallic glass ribbons and for numerous discussions.

References

1. P. G. ZIELINSKI, J. OSTATEK, M. KIJEK and H. MATYJA, Rapidly Quenched Metals, Vol. 1. edited by B. Cantor (The Metals Society, London, 1978) p. 337.
2. H. S. CHEN and J. T. KRAUSE, *Scripta Metall.* **11** (1977) 761.
3. A. INOUE, H. TOMIOKA and T. MASUMOTO, *J. Mater. Sci.* **18** (1983) 153.
4. S. TAKAYAMA and R. MADDIN, *ibid,* **11** (1976) 22.
5. C. P. CHOU and F. SPAEPEN, *Acta Metall.* **23** (1975) 609.
6. H. G. HILLENBRAND, E. HORNBOGEN and U. KÖSTER, Proceedings of the Fourth International Conference on Rapidly Quenched Metals, Sendai, edited by T. Masumoto and K. Suzuki (The Japan Institute of Metals, Sendai, 1982) p. 1369.
7. T. MASUMOTO and R. MADDIN, *Mater. Sci. Eng.* **19** (1975) 1.
8. C. A. PAMPILLO, *J. Mater. Sci.* **10** (1975) 1174.
9. P. E. DONOVAN and W. M. STOBBS, *Acta Metall.* **29** (1981) 1419.
10. S. C. HUANG and H. C. FIEDLER, *Met. Trans.* **12A** (1981) 1107.
11. P. M. SARGENT, *Scripta Metall.* **16** (1982) 1207.
12. L. A. DAVIS, *ibid.* **9** (1975) 431.
13. L. A. DAVIS, N. J. GRANT and B. C. GIESSEN (eds), Proceedings of the Second International Conference on Rapidly Quenched Metals, (Massachusetts Institute of Technology, Cambridge, USA, 1975) p. 369.
14. D. L. DOUGLASS, "The Metallurgy of Zirconium" (International Atomic Energy Agency, Vienna, 1971) p. 229.
15. C. E. ELLS and B. A. CHEADLE, *J. Nucl. Mater.* **23** (1967) 257.

16. P. E. DONOVAN and W. M. STOBBS, *J. Microsc.* **119** (1980) 39.
17. J. P. CHEVALIER, *ibid.* **119** (1980). 45.
18. J. GILMAN, *J. Appl. Phys.* **46** (1975) 1625.
19. H. J. LEAMY, H. S. CHEN and T. T. WANG, *Met. Trans.* **3** (1972) 699.

Received 20 June
and accepted 20 September 1984